

Clathrates of TETROL: Further Aspects of the Selective Inclusion of Methylcyclohexanones in Their Energetically Unfavorable Axial Methyl Conformations

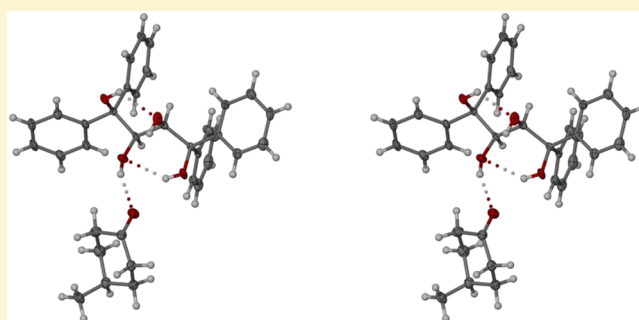
Benita Barton,* Mino R. Caira,*[†] Eric C. Hosten, Cedric W. McClelland, and Selwyn Weitz

Department of Chemistry, Nelson Mandela Metropolitan University, PO Box 77000, Port Elizabeth, 6031, South Africa

[†]Department of Chemistry, University of Cape Town, Rondebosch, 7701, South Africa

S Supporting Information

ABSTRACT: (+)-(2*R*,3*R*)-1,1,4,4-Tetraphenylbutane-1,2,3,4-tetraol (TETROL) functions as a highly efficient host for the inclusion of cyclohexanone and 2-, 3-, and 4-methylcyclohexanone, all with 1:1 host/guest ratios. Most extraordinarily, the 3- and 4-methyl isomers are uniquely included in their higher energy axial methyl conformations rather than as their more energetically favorable equatorial analogues. In contrast, 2-methylcyclohexanone is included more conventionally in the equatorial methyl conformation. During recrystallization of TETROL from racemic 2- and 3-methylcyclohexanone, some preference is shown by the host for the (*R*)-enantiomer. In the latter case, this is attributed to a much stronger H-bond between a hydroxyl group of TETROL and the carbonyl group of the (*R*)-enantiomer (O...O 2.621(2) Å) compared with a significantly weaker H-bond to the (*S*)-enantiomer (3.125(8) Å). In the former instance, hydrogen-bond strengths to both enantiomers are similar, but the (*R*)-enantiomer engages in three (guest)CH... π (host) and three (guest)H...C_{ar}(host) contacts, whereas fewer interactions of these types are observed for the (*S*)-enantiomer. Calculations of geometries of the guest cyclohexanones were determined at the MP2/6-311++G(2df,2p) level and compared with those obtained at the G3(MP2) level. Finally, an interesting correlation between crystal packing indices for the three methylcyclohexanone clathrates and their respective desolvation onset temperatures was identified.



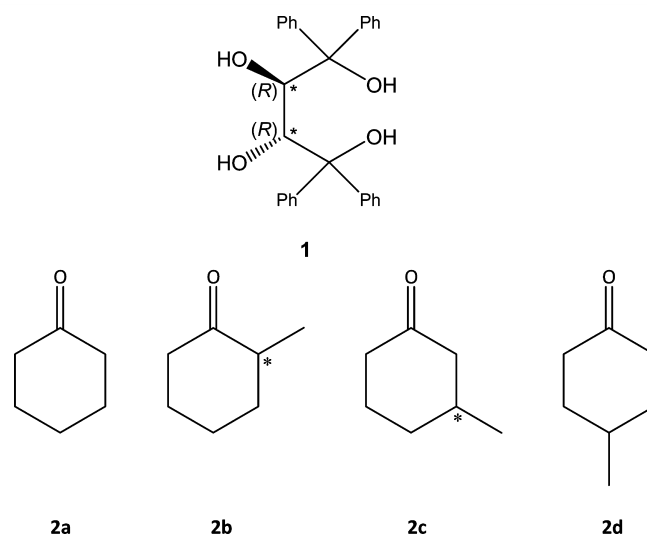
1. INTRODUCTION

We have reported that TETROL, (+)-(2*R*,3*R*)-1,1,4,4-tetraphenylbutane-1,2,3,4-tetrol **1**, functions as an efficient and novel clathrate host, and this was demonstrated by its ability to discriminate between pyridine derivatives.¹ As TETROL is chiral, it has the potential for stereoselective inclusion of guest compounds, similar to that with the structurally related TADDOLs.² We subsequently reported as a short communication³ that TETROL enclathrates cyclohexanone **2a** as well as the isomeric 2-, 3-, and 4-methylcyclohexanones (**2b**, **2c**, and **2d**), with **2c** and **2d** in their energetically unfavorable axial methyl conformations. This article elaborates these findings further.

2. RESULTS AND DISCUSSION

TETROL **1** was prepared by reacting phenyl magnesium bromide with optically active (+)-diethyl L-tartrate using standard Grignard reaction methodology.¹

2.1. Formation of Inclusion Complexes. TETROL **1** was dissolved with heating in cyclohexanone and 2-, 3-, and 4-methylcyclohexanone **2a–2d** individually. These guest solvents were allowed to evaporate at ambient temperature and pressure, and crystallization ensued. The crystals were collected, washed thoroughly with petroleum ether, and dried under suction filtration. ¹H NMR experiments were conducted on the resultant



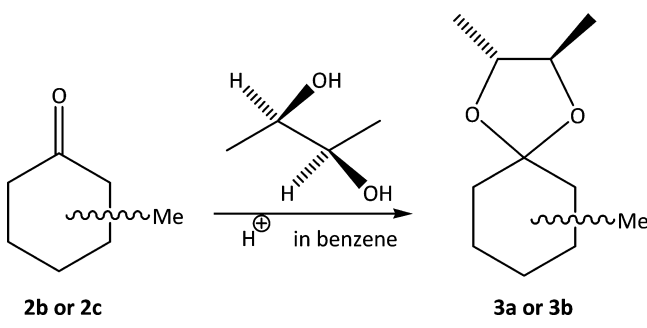
solids to determine whether inclusion had occurred and, if so, the host/guest (H/G) ratios. All four cyclohexanones formed inclusion complexes in this way, each with a 1:1 H/G ratio.

Received: May 13, 2015

Published: June 11, 2015

2.2. Enantioselectivity in Enclathration of Racemic 2- and 3-Methylcyclohexanone by TETROL. The complexes obtained when 2- and 3-methylcyclohexanone (**2b** and **2c**, respectively) were enclathrated were analyzed in order to determine whether **1** manifested any enantioselectivity. This was accomplished by distilling each of the guests out of the host crystal under vacuum and reacting the respective distillates with (2*R*,3*R*)-(-)-butane-2,3-diol in the presence of an acid catalyst to give diastereomeric acetals **3a** (from 2-methylcyclohexanone) and **3b** (from 3-methylcyclohexanone) (Scheme 1).

Scheme 1. Synthesis of Diastereomeric Acetals 3a and 3b from 2- and 3-Methylcyclohexanone, 2b and 2c, Respectively



These diastereomers were analyzed by ^{13}C NMR spectroscopy, where the percentage enantiomeric excess (% ee) was calculated from the integrals of the respective twinned ^{13}C signals arising in the pairs of diastereoisomers formed in each case (Figure 1a,b). Lemière et al.⁴ have reported on the determination of absolute configurations of six-membered ring ketones in this way. Using their technique, we established that TETROL has a preference for the (*R*)-enantiomers for both 2- and 3-methylcyclohexanone (Tables 1 and 2).

Table 1 shows both our observed and Lemière's reported C-13 chemical shifts, which are in close agreement. Table 2 gives the calculated ee's, with the (*R*)-enantiomer being preferred in both cases.

2.3. Single-Crystal X-ray Diffraction Analyses of the 1·2a, 1·2b, 1·2c, and 1·2d Inclusion Complexes. Crystal data and refinement parameters are listed in Table 3, and the respective asymmetric units are illustrated in Figure 2. It is evident that the conformation of the TETROL molecule is primarily determined by intramolecular O–H...O hydrogen bonding, as reported previously,¹ and that it is fairly constant throughout this series of inclusion complexes.

Figure 2 also displays the primary host–guest interaction in the four complexes, namely, a hydrogen bond (host)O–H...O(guest), that links a common hydroxyl group of the TETROL molecule to the respective guest carbonyl oxygen atom. The O...O distances for the host–guest H-bonds in **1·2a** and **1·2d**, containing achiral methylcyclohexanones, are not significantly different (2.716(2) and 2.713(4) Å, respectively). However, in **1·2b** and **1·2c**, each chiral guest molecule is disordered, occurring as two enantiomers, with the (*R*)-enantiomer consistently being the major one; for the single crystals analyzed, the site-occupancy factors (sof) for the (*R*)- and (*S*)-enantiomer are 0.65 and 0.35 in **1·2b** and 0.78 and 0.22 in **1·2c**, respectively. There are thus two unique hydrogen-bonded host–guest O...O distances in **1·2b** (2.716(2), 2.705(6) Å, which are not significantly different), as well as in **1·2c** (2.621(2), 3.125(8) Å, which, however, are significantly different). In the latter case, the shorter O...O

distance, reflecting much stronger hydrogen bonding, is associated with the guest (*R*)-enantiomer, which has the higher sof of 0.78. Preference for inclusion of the guest (*R*)-enantiomers established from X-ray analyses of **1·2b** and **1·2c** is consistent with the conclusion based on the NMR spectroscopic analyses of the diastereomeric acetals described above.

Also evident from Figure 2 is that the enclathrated 3-methylcyclohexanone and 4-methylcyclohexanone molecules in the respective inclusion crystals **1·2c** and **1·2d** adopt the energetically unfavorable axial methyl conformations. As we reported recently,³ this is the most remarkable feature of this pair of inclusion complexes and one which therefore warranted careful investigation. The unprecedented occurrence of these atypical guest conformations was subsequently rationalized on the basis of the presence of multiple, cooperative (guest)CH... π (host) and (guest)H...C_{ar}(host) stabilizing interactions, which complement the anchoring role of the (host)O–H...O(guest) hydrogen bonds (Figure 3).

In the crystal of **1·2c**, stabilization of the axial methyl conformer of the (major) (*R*)-enantiomer of 3-methylcyclohexanone was found to be mediated by three (guest)CH... π (host) interactions and a short (guest)H...C_{ar}(host) interaction (Figure 3, left), whereas stabilization of the axial conformer of the (minor) (*S*)-enantiomer was attributed to three (guest)CH... π (host) interactions and three weaker attractive (guest)H...C_{ar}(host) interactions. In the crystal of **1·2d**, containing 4-methylcyclohexanone, the observed axial methyl conformation was ascribed to stabilization via two (guest)CH... π (host) interactions and four (guest)H...C_{ar}(host) interactions (Figure 3, right). Full geometrical data for these interactions were reported in the previous communication.³

In contrast to the above findings, the 2-methylcyclohexanone molecule in complex **1·2b** is present as the equatorial methyl conformer. Figure 4, illustrating inclusion of the (*R*)-enantiomer, shows that the equatorial conformation is also stabilized by the types of host–guest interactions mentioned above (specifically, three (guest)CH... π (host) and three attractive (guest)H...C_{ar}(host) interactions). Geometrical data appear in the Supporting Information.

It is noteworthy that the (guest)CH... π (host) interaction (3) involves the tertiary H atom at the chiral center of **2b**. An analogous figure for enclathration of the (*S*)-enantiomer in the **1·2b** crystal (see the Supporting Information) features only one (guest)CH... π (host) interaction and two (guest)H...C_{ar}(host) interactions, which is consistent with its lower sof in the crystal, reflected also in the NMR-based analytical data (Table 2).

2.3.1. Crystal Packing. The crystal packing in the four complexes was investigated in some detail to gauge the rigidity of the host frameworks and the modes of encapsulation of the respective guest molecules, with a view to eventually correlating these features with the results of thermal analysis. In all cases, the guest molecules were found to occupy isolated cavities within their respective host matrices, with the common equivalent of one guest molecule per cavity. Figure 5 shows the topology of the isolated cavities in the crystals of **1·2a** and **1·2b** occupied by the cyclohexanone and 2-methylcyclohexanone molecules, respectively. Analogous cavities occurring in inclusion complexes **1·2c** and **1·2d** were described earlier.³

Crystal packing diagrams are shown in Figure 6. It has been noted that the inclusion complexes containing cyclohexanone (**1·2a**) and 3-methylcyclohexanone (**1·2c**) crystallize in the same space group with very similar unit cell dimensions, from which it was deduced that their host frameworks are isostructural. This is

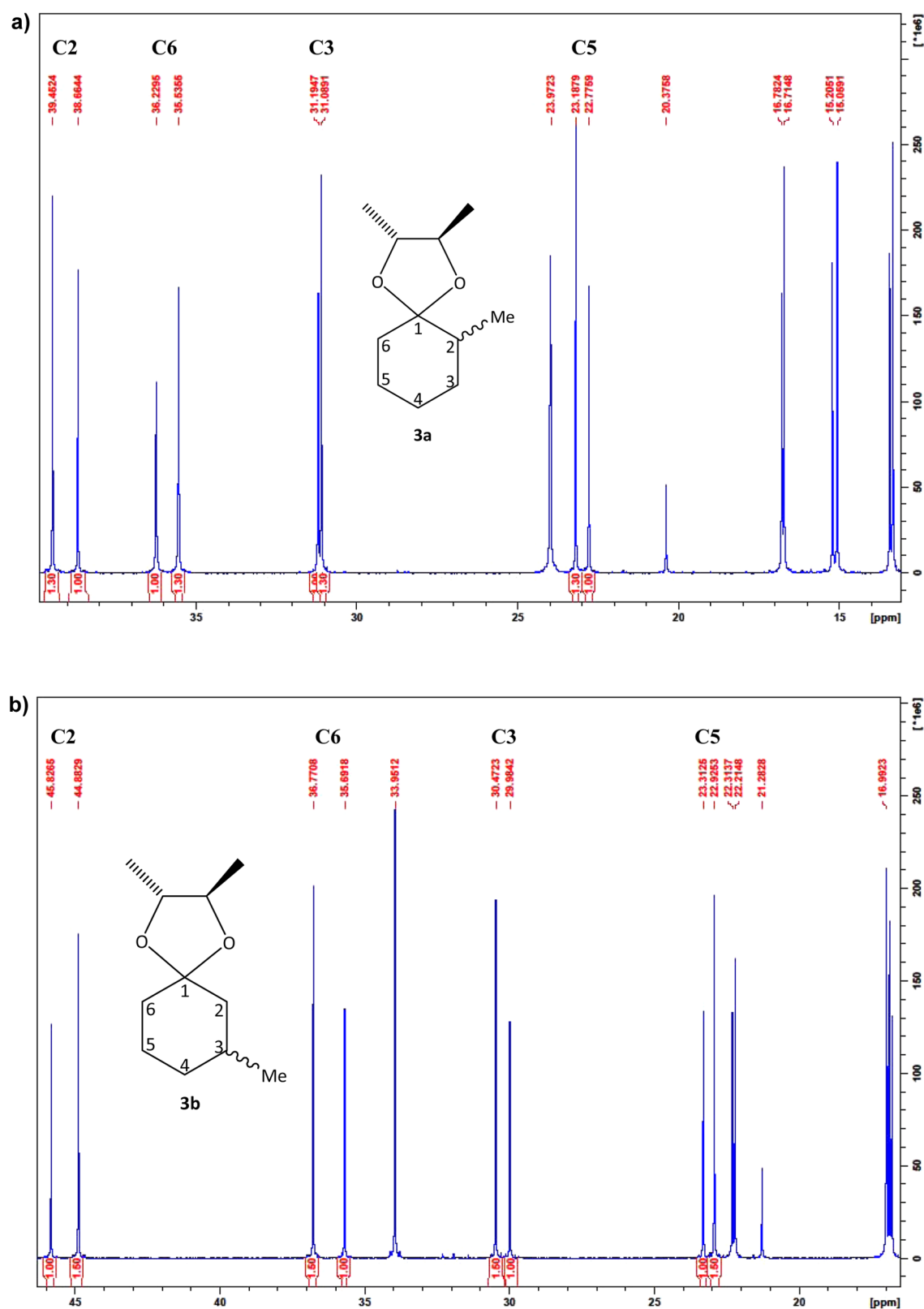


Figure 1. (a) Upfield ^{13}C NMR spectrum of diastereomeric acetals (a) **3a** and (b) **3b** formed from 2-methylcyclohexanone.

strikingly evident from Figure 6 and the isostructurality is also confirmed by the close match of the simulated PXRD patterns for these two crystals (see the Supporting Information).

For each of the crystals, **1·2a**, **1·2c**, and **1·2d**, the hydrogen bonds include the intramolecular O–H \cdots O bonds in the

TETROL molecule and the O–H \cdots O bond between the host and guest molecules. Thus, there are no strong host–host interactions and a search for weaker host π – π stacking showed no interaction of this kind with phenyl ring centroids less than 4.7 Å apart. Only in the crystal of **1·2b** is there some level of

Table 1. ^{13}C Chemical Shifts (ppm) for Selected Carbon Atoms in Acetals 3a and 3b^a

compd	C2	C3	C5	C6
(R)-3a	39.45 (40.42)	31.10 (32.11)	23.19 (24.20)	35.54 (36.53)
(S)-3a	38.66 (39.64)	31.19 (32.21)	22.78 (23.79)	36.23 (37.23)
(R)-3b	44.88 (44.98)	30.47 (30.61)	22.93 (23.05)	36.77 (36.89)
(S)-3b	45.83 (45.91)	29.98 (30.12)	23.31 (23.44)	35.69 (35.82)

^aThe numbering sequence for ring carbon atoms is shown in Figure 1a,b; Lemièrè's values⁴ are given in parentheses.

Table 2. Enantiomeric Excesses for Acetals 3a and 3b

compd	relative area of integral for C2	% enantiomer prevalence in the mixture	% enantiomeric excess of (R)-enantiomer
(R)-3a	1.30	56.52	13.04%
(S)-3a	1.00	43.48	
(R)-3b	1.50	60.00	20.00%
(S)-3b	1.00	40.00	

host–host cohesion via classical O–H...O hydrogen bonding. Specifically, the TETROL molecules are linked head-to-tail by a O–H...O bond (O...O 2.774(2) Å) between the terminal hydroxyl groups of molecules related by the 2_1 -axis parallel to the crystal axis *a*. They thus form infinite chains propagating in the crystal *x*-direction, which serve to strengthen the host framework relative to those in the other complexes. However, again, no π – π stacking is evident.

Guest enclathration within isolated voids often results in high thermal stability of the crystals of the inclusion compound,⁵ but for the present series, the onset temperatures for crystal

desolvation determined by thermogravimetry span a relatively low range of ~50–80 °C, which (except in the case of 1·2b) we attribute to the general lack of cohesion among the enclathrating host molecules.

2.4. Computational Studies. The conformational equilibria for monosubstituted alkyl cyclohexanes are unvaryingly biased in favor of chair conformers bearing the alkyl group in the equatorial position. However, for 3-alkyl-cyclohexanones, the conformational free energy differences are significantly smaller, and this results in higher relative amounts of the axial conformers, although the equatorial isomers still dominate. This 3-alkylketone effect⁶ has been attributed to the removal of one of the destabilizing 1,3-diaxial alkyl-hydrogen van der Waals repulsions as a result of replacing a tetrahedral 3-methylene carbon with the trigonal planar carbon of the carbonyl group. Accordingly, the equatorial – axial enthalpy difference has been estimated to be approximately 2.5 kJ mol⁻¹ smaller.⁷

We observed previously that for the (R)-enantiomer of 3-methylcyclohexanone in the crystal of 1·2c the remaining

Table 3. Crystallographic Data for 1·Cyclohexanone and 1·2-, 1·3-, and 1·4-Methylcyclohexanone

	1·cyclohexanone	1·2-methylcyclohexanone	1·3-methylcyclohexanone	1·4-methylcyclohexanone
chemical formula	C ₂₈ H ₂₆ O ₄ ·C ₆ H ₁₀ O	C ₂₈ H ₂₆ O ₄ ·C ₇ H ₁₂ O	C ₂₈ H ₂₆ O ₄ ·C ₇ H ₁₂ O	C ₂₈ H ₂₆ O ₄ ·C ₇ H ₁₂ O
formula weight	524.63	538.65	538.65	538.65
crystal system	monoclinic	orthorhombic	monoclinic	triclinic
space group	<i>P</i> 2 ₁	<i>P</i> 2 ₁ 2 ₁ 2 ₁	<i>P</i> 2 ₁	<i>P</i> 1
μ (Mo K α)/mm ⁻¹	0.084	0.082	0.083	0.084
<i>a</i> /Å	12.5944(4)	10.3843(3)	12.4493(6)	8.181(2)
<i>b</i> /Å	8.1531(2)	15.2193(3)	8.2368(4)	9.952(3)
<i>c</i> /Å	13.4570(5)	18.2734(4)	13.9466(7)	10.163(3)
α /deg	90	90	90	79.296(6)
β /deg	94.025(2)	90	95.843(2)	68.813(5)
γ /deg	90	90	90	65.825(5)
<i>V</i> /Å ³	1378.40(8)	2887.96(12)	1422.69(12)	703.2(3)
<i>Z</i>	2	4	2	1
<i>F</i> (000)	560	1152	576	288
temp.	200	200	200	173
restraints	1	0	9	3
<i>N</i> _{ref}	6501	6716	6823	9403
<i>N</i> _{par}	356	440	399	366
<i>R</i>	0.0388	0.0335	0.0459	0.0515
<i>wR</i> ₂	0.1045	0.0862	0.1354	0.1338
<i>S</i>	1.04	1.03	1.04	0.94
θ min, max/deg	1.5, 28.3	1.7, 28.3	2.1, 28.3	2.2, 27.1
tot. data	13 345	15 292	26 618	9415
unique data	6501	6716	6823	9403
observed data	5556	6013	6031	5729
[<i>I</i> > 2.0 σ (<i>I</i>)]				
<i>R</i> _{int}	0.017	0.012	0.014	0.000
dffrms measured	1.000	0.999	0.996	0.952
fraction θ full				
min. resd. dens. (e/Å ³)	-0.21	-0.17	-0.27	-0.25
max. resd. dens. (e/Å ³)	0.22	0.22	0.28	0.26

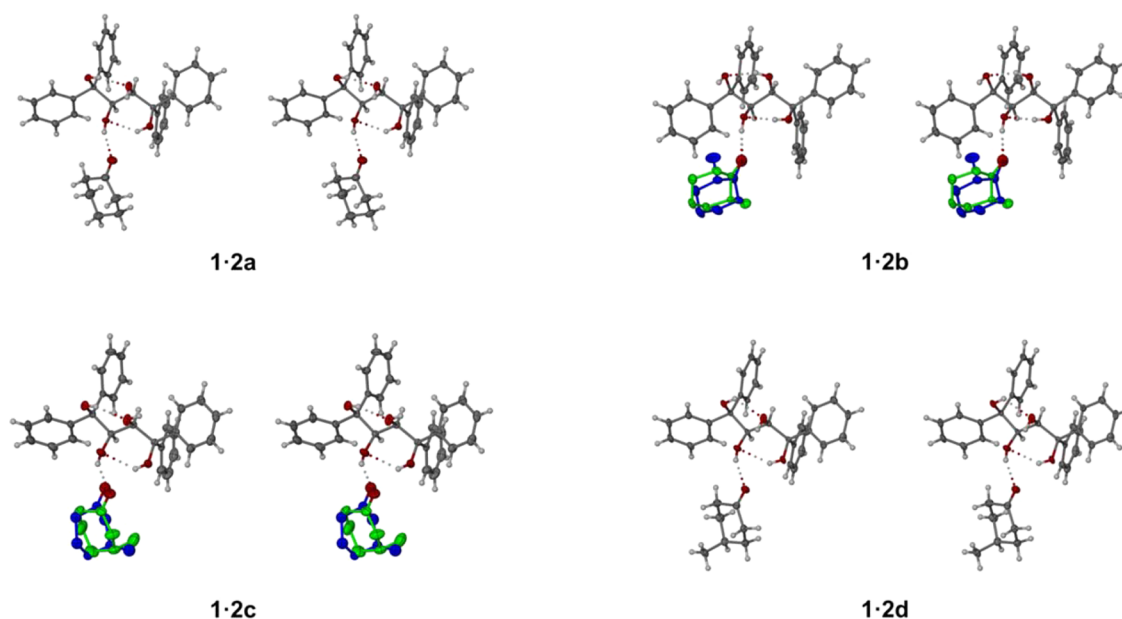


Figure 2. Stereoviews of the asymmetric units in the crystals of the four inclusion complexes; guest H atoms in **1·2b** and **1·2c** have been omitted for clarity, and their respective components of guest disorder are colored green (*R*-) and blue (*S*-); thermal ellipsoids are drawn at the 40% probability level.

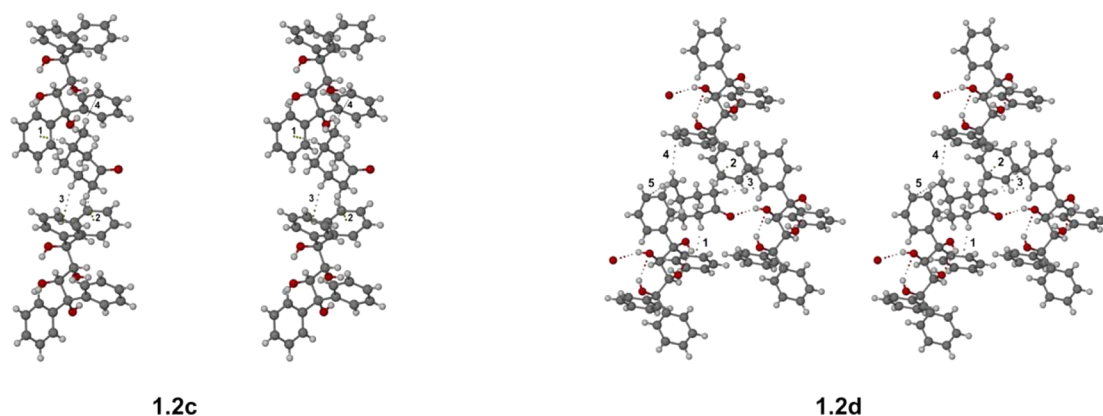


Figure 3. Stereoview illustrating interactions stabilizing the axial conformer of the (*R*)-enantiomer of 3-methylcyclohexanone in the crystal of **1·2c** (left) and the axial conformer of 4-methylcyclohexanone in the crystal of **1·2d**.³

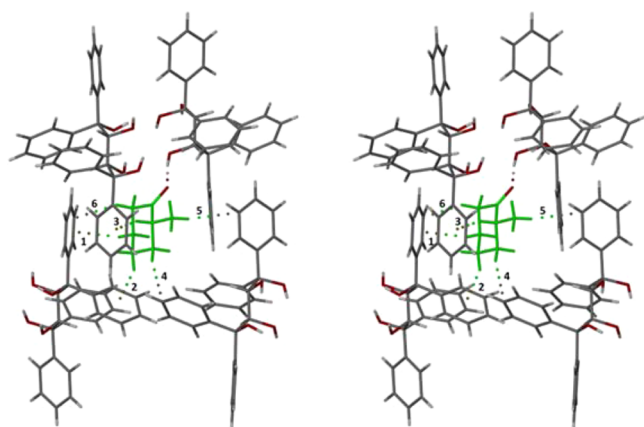


Figure 4. Stereoview illustrating the interactions that stabilize the equatorial conformer of the guest (*R*)-enantiomer in the **1·2b** complex crystal; labels 1–3 designate (guest)CH \cdots π (host) interactions and 4–6, attractive (guest)H \cdots C_{ar}(host) interactions; the host–guest O–H \cdots O hydrogen bond is also shown.

1,3-diaxial repulsive interaction is not significant since the methyl group orientation is such that its two closest H atoms are sufficiently far from the syn axial methylene H atom, with distances measuring 2.4 and 2.8 Å. Stabilization of the axial conformer is attributed to an attractive intramolecular CH/ π (C=O) interaction that involves the closest methyl H atom (H \cdots C distance 2.65 Å). This is reinforced by *ab initio* calculations at the MP2/6-311++G(d,p)//MP2/6-311G(d,p) level performed by Takahashi et al.,⁸ who ascribed the alkylketone effect in axial 2- and 3-alkyl-cyclohexanones to a stabilizing interaction of this kind.

We previously reported³ on G3(MP2) composite calculations on the series of isomeric methylcyclohexanones as well as methylcyclohexane, where similar trends to those reported by Takahashi and co-workers⁸ were observed. The general preference for the equatorial conformers was confirmed, as was a significant 3-alkylketone effect for 3-methylcyclohexanone **2c**.

We now report on calculations we performed on these species at the MP2/6-311++G(2df,2p) level, with geometry optimization in all cases (Table 4).

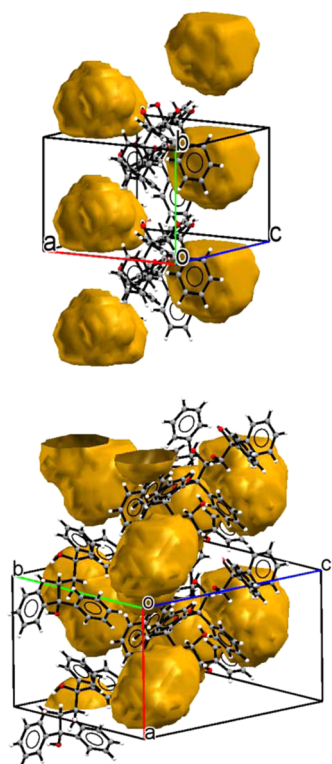


Figure 5. Guest-containing cavities in the crystals of **1·2a** (top) and **1·2b** (bottom).

Compared to the G3(MP2) composite method where geometry optimization is limited to the MP2(full)/6-31G* level, followed with MP2, MP4, and QCISD(T) single-point energy determinations, similar energy trends were obtained from the MP2/6-311++G(2df,2p) calculations, except that the magnitudes of both the 2- and 3-alkylketone effects were found to be comparatively larger in the latter case.

In our earlier communication,³ we also compared in detail the structures of the three methyl cyclohexanone conformers found in the host–guest complexes, with the corresponding geometries computed at the G3(MP2) level. In each case, the precision of the fit obtained when C and O atom pairs in the crystal and computed structures were aligned was determined by calculating the resulting root-mean-square deviations (rmsd) for the overlay. Similar comparisons have now been made between the theoretical MP2/6-311++G(2df,2p) and crystal structures (Table 5).

Interestingly, closer structural correspondences with the crystal structures were found for the G3(MP2) compared to MP2/6-311++G(2df,2p) theoretical structures, even though a substantially larger basis set incorporating diffuse and polarization functions for all the atoms was used in the latter case. This effect could be anomalous since it is possible that the geometries of conformers **2b_{eq}**, **2c_{ax}**, and **2d_{ax}** could be somewhat distorted through the influence of their crystal structure environments. However, it has been noted that the smaller 6-31G* basis set is particularly robust and generally provides theoretical geometries that compare favorably with experimental structures.⁹ Although

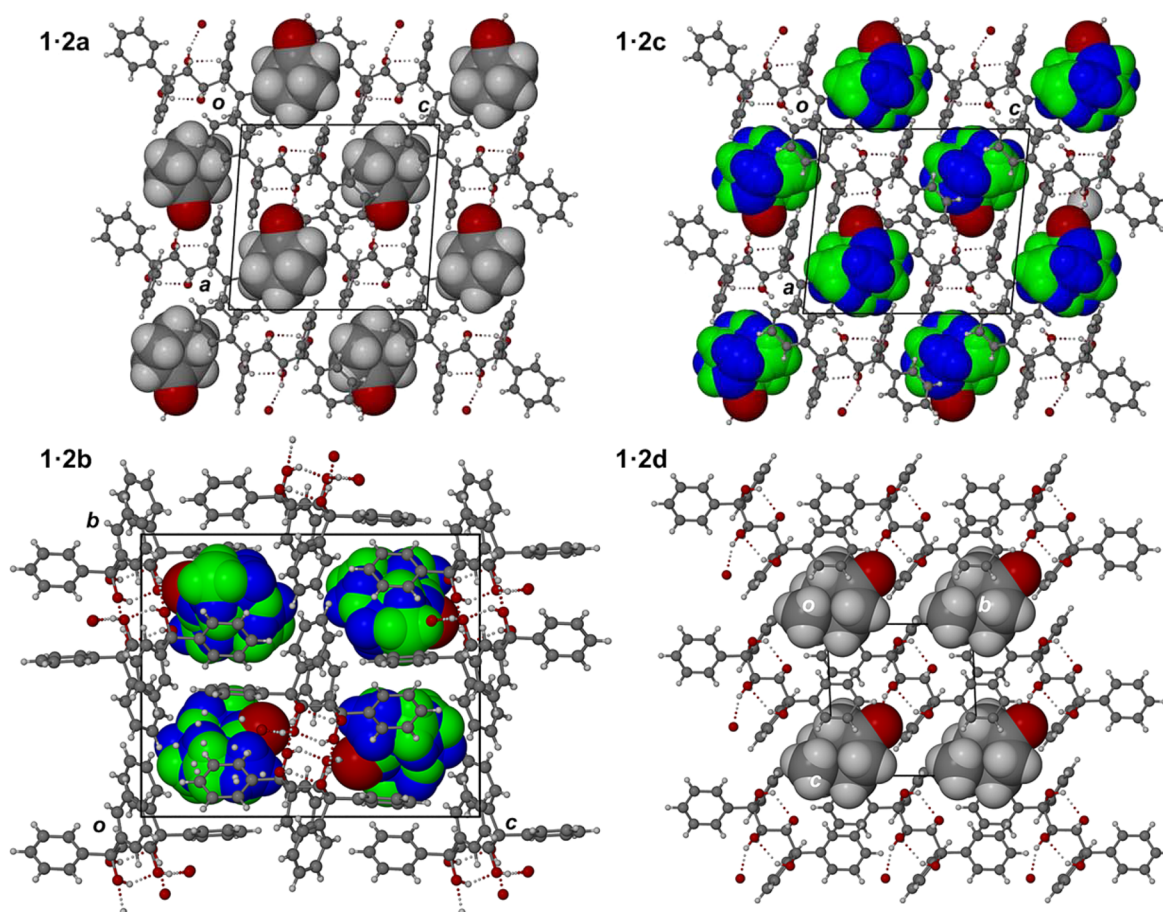


Figure 6. Crystal packing in the four inclusion complexes; host atoms are shown in ball-and-stick representation, and the guest molecules, in space-filling mode; guest enantiomers in **1·2b** and **1·2c** are colored green (*R*-) and blue (*S*-).

Table 4. Computed Free Energies^a (kJ mol⁻¹) and Conformer Boltzmann Distributions for Methylcyclohexanones 2b–2d and Methylcyclohexane 4

	2b	2c	2d	4
Equatorial Conformers	2b_{eq}	2c_{eq}	2d_{eq}	4_{eq}
ΔG_{eq}	-914455.01 (0.39) ^b	-914455.40 (0.00)	-914455.09 (0.31)	-720316.54
Axial Conformers	2b_{ax}	2c_{ax}	2d_{ax}	4_{ax}
ΔG_{ax}	-914447.94 (7.46)	-914451.22 (4.18)	-914448.51 (6.58)	-720308.63
$\Delta G_{ax} - \Delta G_{eq}$	7.07	4.18	6.58	7.90
Boltzmann Distributions				
equatorial	0.945	0.844	0.934	0.960
axial	0.055	0.156	0.066	0.040
Alkyl Ketone Effect ^c				
MP2/6-311++G(2df,2p)	0.84	3.72	1.32	
G3(MP2) ³	0.12	3.25	1.33	

^aMP2/6-311++G(2df,2p) with geometry optimization. ^bRelative to the lowest energy methyl-cyclohexanone conformer (2c_{eq}). ^c($\Delta G_{ax} - \Delta G_{eq}$)_{methylcyclohexane} - ($\Delta G_{ax} - \Delta G_{eq}$)_{methylcyclohexanone}.

Table 5. RMSD Values (Å) for the Least-Squares Fit of C and O Atom Pairs in the Crystal and Computed Structures for Equatorial 2-Methylcyclohexanone (2b_{eq}), Axial 3-Methylcyclohexanone (2c_{ax}), and Axial 4-Methylcyclohexanone (2d_{ax})

	2b _{eq}	2c _{ax}	2d _{ax}
G3(MP2) ³	0.029	0.093	0.072
MP2/6-311++G(2df,2p)	0.034	0.092	0.082

accurate descriptions of equilibrium structures for molecules containing heteroatoms using MP2 models require polarization basis sets, statistical analysis has shown that the errors associated with the 6-31G* basis set are generally comparable to those of significantly larger basis sets such as 6-311+G**.

2.5. Thermal Stability Analyses. Thermal experiments (DSC and TG) were carried out on the four formed inclusion complexes. The traces obtained from these experiments are given in Figure 7a–d, which were the results of the powdered complexes being heated at a constant rate of 5 K min⁻¹ from approximately 25–30 °C to between 170 and 300 °C. (The traces have been rescaled for clarity.)

Upon heating the cyclohexanone complex, an intricate and stepwise guest release process follows (Figure 7a), ultimately culminating in the host melt coinciding with the last of the guest being liberated (the endotherm peaking at 142.9 °C). The expected mass loss for a 1:1 H/G complex was calculated to be 18.7%, which is in reasonable agreement with that observed (17.5%, Table 6). A similarly complex process is seen for

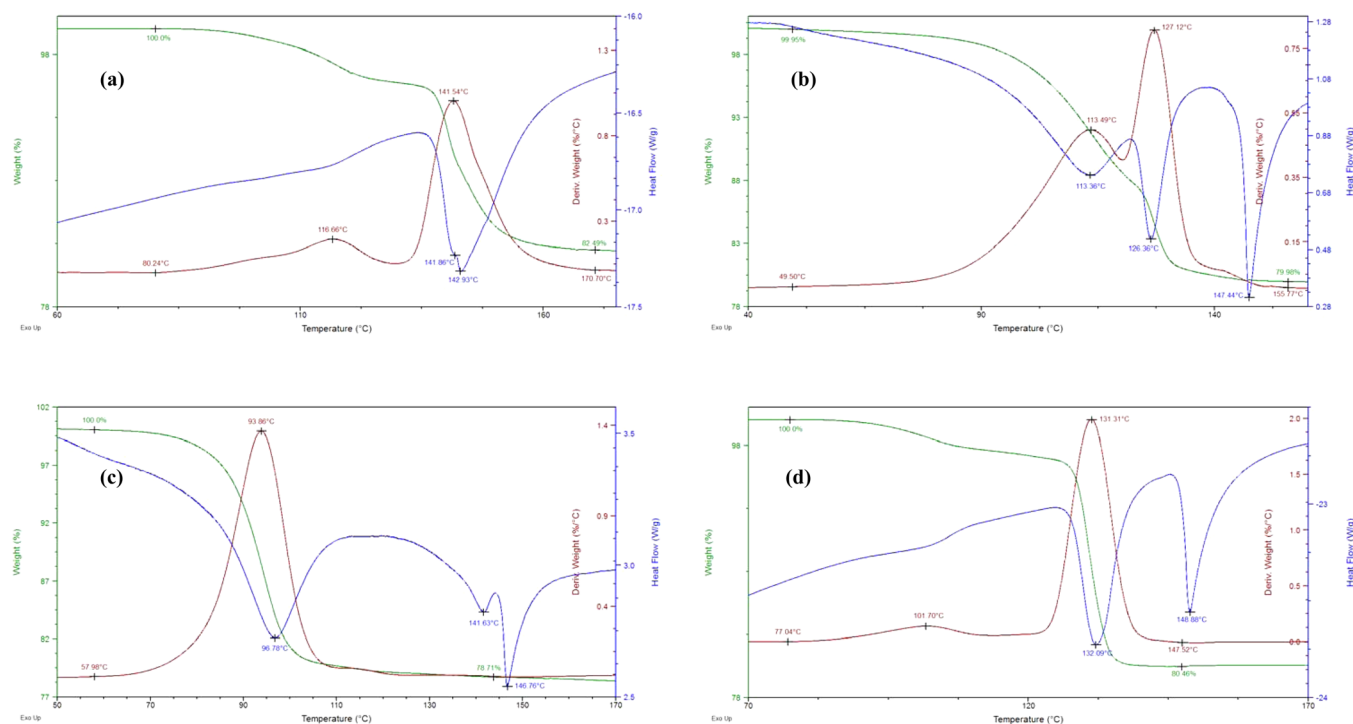
**Figure 7.** Overlaid traces of the DSC (blue), TG (green), and its derivative (brown) for the (a) TETROL-cyclohexanone complex, (b) TETROL-2-methylcyclohexanone complex, (c) TETROL-3-methylcyclohexanone complex, and (d) TETROL-4-methylcyclohexanone complex.

Table 6. Thermal Data from DSC/TG Analysis of 1·2a, 1·2b, 1·2c, and 1·2d

guest	$T_{\text{on}}/^{\circ}\text{C}^a$	observed mass loss (%)	expected mass loss (%)
cyclohexanone (2a)	80.2	17.5	18.7
2-methylcyclohexanone (2b)	49.5	20.0	20.8
3-methylcyclohexanone (2c)	58.0	21.3	20.8
4-methylcyclohexanone (2d)	77.0	19.5	20.8

^a T_{on} , the onset temperature for the guest release process, was estimated from the TG derivatives (brown curves, Figure 7a–d).

1·2-methylcyclohexanone (Figure 7b), but here the majority of the guest is released prior to the melting of the host (147.4 °C). The leaving of 3-methylcyclohexanone molecules from the host cavities appears to be much less convoluted than in the previous two instances, and most of the guest is liberated in a single step (Figure 7c). The inflection (the endotherm peaking at 141.6 °C) just prior to the melting of the host (146.8 °C) is most likely due to a phase change occurring in the host, since there is no mass loss associated with this endotherm. Finally, heating the TETROL·4-methylcyclohexanone complex leads to stepwise guest release (Figure 7d), although this process is much simpler than that for the 2-methylcyclohexanone complex, and the host melt occurs at 148.9 °C (peak value). In the last three complexes, the observed mass losses (20.0, 21.3, and 19.5%, Table 6) are in close agreement with those expected for 1:1 complexes (20.8%).

Packing indices for the inclusion compounds containing the three methylcyclohexanone isomers were calculated as 0.68, 0.69, and 0.70 for 1·2b, 1·2c and 1·2d, respectively. These values correlate with the increasing trend in the respective crystal desolvation onset temperatures listed in Table 6, leading to the conclusion that more efficient crystal packing leads to a thermally more stable clathrate.

3. CONCLUSIONS

TETROL has shown the unique ability to include 3- and 4-methylcyclohexanone solely as their high energy axial conformers. Two other alicyclic ketones, cyclohexanone and 2-methylcyclohexanone, are also included by this host, and all complexes are formed with 1:1 H/G ratios. Discrimination between the enantiomers of racemic 2- and 3-methylcyclohexanone was observed with the (R)-enantiomer preferentially selected by the host in both cases. The guests always occupy discrete cavities in the host crystal, but this did not result in complexes of significantly high thermal stabilities (T_{on} ranged between 50 and 80 °C); this was ascribed to the lack of any significant intermolecular host–host interactions (with the exception of 2-methylcyclohexanone). The geometries of the guest cyclohexanones found in the crystal structures compared favorably with those obtained from molecular orbital calculations.

We have now reported on examples where TETROL (which is structurally related to the TADDOLs) displays unique host properties in host–guest compounds. We envisage further applications in the field of chromatographic racemate separations, as well as asymmetric synthesis, and will report on our findings in due course.

4. EXPERIMENTAL SECTION

4.1. General. Melting points are uncorrected. Infrared spectra were recorded using an ATR-FTIR system, and ¹H and ¹³C NMR spectra were obtained using a 400 MHz spectrometer. Samples for DSC and TG experiments were placed in open ceramic pans with an empty ceramic pan functioning as a reference. High-purity nitrogen gas was used

as purge gas. Optical rotations were measured using a polarimeter equipped with a sodium lamp.

4.2. Synthesis of (+)-(2R,3R)-1,1,4,4-Tetraphenylbutane-1,2,3,4-tetraol 1. This compound was synthesized according to a published procedure.¹ This afforded a gum that was crystallized and recrystallized from CH₂Cl₂/hexane/MeOH to afford (+)-(2R,3R)-1,1,4,4-tetraphenylbutane-1,2,3,4-tetraol **1** as a white solid (45%), mp 147–149 °C (lit.,¹⁰ mp 150–151 °C); [α]_D²³ = +166 (c 9.32, CH₂Cl₂) {lit.,¹⁰ [α]_D²⁵ = +154 (c 1.2, CHCl₃)}; ν_{max} (solid)/cm⁻¹ 3440 (br, OH), 3294 (br, OH), 3057 (Ar), 3033 (Ar), 1598 (Ar), and 1494 (Ar); δ_{H} (CDCl₃) 3.86 (2H, d, 2COH), 4.44 (2H, d, 2HCOH), 4.72 (2H, s, 2CPh₂OH), and 7.2–7.4 (20H, m, Ar); δ_{C} (CDCl₃) 72.1 (HCOH), 81.7 (CPh₂OH), 125.0 (Ar), 126.1 (Ar), 127.1 (Ar), 127.3 (Ar), 128.4 (Ar), 128.6 (Ar), 143.9 (quaternary Ar), and 144.2 (quaternary Ar).

4.3. Computational Studies. Calculations were performed using SPARTAN '10 for Windows [build 1.1.0 (Mar 20, 2011)] software, supplied by Wavefunction Inc. Preliminary structures were determined using the MMFF (Merck Pharmaceuticals) force field, followed by further geometry refinement at the DFT level using the B3LYP functional and progressively employing the 6-31G*, 6-311++G**, and 6-311++G(2df,2p) basis sets. Thermochemical calculations were carried out at the G3(MP2) and MP2/6-311++G(2df,2p) levels, with the former approach providing standard enthalpies of formation, and the latter, total Gibbs free energies at 298.15 K and 1 atm of pressure.

Least-squares overlays of pairs of crystal and computed structures were performed using the Structure Overlay function in Mercury CSD 3.5.1 (build RCS) provided by the Cambridge Crystallographic Data Centre (CCDC).

4.4. Single-Crystal X-ray Diffraction. X-ray diffraction studies of the inclusion complexes were performed at 173 or 200 K using a Bruker Kappa Apex II diffractometer with graphite-monochromated Mo K α radiation ($\lambda = 0.71073$ Å). APEXII¹¹ was used for data collection, and SAINT,¹¹ for cell refinement and data reduction. The structures of 1·2a, 1·2b, and 1·2c were solved routinely by direct methods using SHELXS-97¹² and refined by least-squares procedures using SHELXL-97¹² with ShelXle¹³ as a graphical interface. Crystals of 1·2d consistently displayed nonmerohedral twinning. For the best specimen selected for analysis, the correct unit cell and orientation matrix were determined using the program CELL_NOW,¹⁴ with the second twin domain being located and indexed by appropriate rotation of the cell. All non-hydrogen atoms were refined anisotropically except those of the (S)-enantiomer of guest 2c owing to its low site occupancy of only 0.22. C-bound H atoms were placed in calculated positions and refined as riding atoms, with C–H 1.00 (CH), 0.95 (aromatic CH), and 0.98 (CH₃) Å and with $U(\text{H}) = 1.2(1.5 \text{ for methyl})U_{\text{eq}}(\text{C})$. The H atoms of the methyl groups were allowed to rotate with a fixed angle around the C–C bond to best fit the experimental electron density (HFIX 137 in the SHELX program suite¹²). The H atoms of the hydroxy groups were allowed to rotate with a fixed angle around the C–O bond to best fit the experimental electron density (HFIX 148 in the SHELX program suite¹²) with $U(\text{H})$ set to $1.5U_{\text{eq}}(\text{O})$. Data were corrected for absorption effects using the multiscan method implemented in SADABS.¹¹ In the absence of significant anomalous scattering, Friedel pairs were merged and the absolute structure was assigned by reference to an unchanging chiral center in the synthetic procedure.

For the final refinement of the twinned structure 1·2d, the SHELXL-97 instructions HKLF 5, MERG 0, and BASF 0.45 were employed, the latter refining to 0.422(2).

■ ASSOCIATED CONTENT

📄 Supporting Information

Stereoviews and crystal data for both the (R)- and (S)-enantiomers of 2-methylcyclohexanone in the TETROL crystal; computed powder diffraction patterns for 1·2a and 1·2c; ¹³C and DEPT-135 NMR spectra; and .cif files for all four complexes [CCDC 989251 (1·2a), 989081 (1·2b), 989004 (1·2c) and 1007403 (1·2d)]. The Supporting Information is available free of charge on the ACS Publications website at DOI: 10.1021/acs.joc.5b01067.

AUTHOR INFORMATION

Corresponding Authors

*(B.B.) Tel: +27 41 504 4859. Fax: +27 41 504 4236. E-mail: benita.barton@nmmu.ac.za.

*(M.R.C.) Tel: +27 21 650 3071. Fax: +27 21 689 7499. E-mail: mino.caira@uct.ac.za.

Notes

The authors declare no competing financial interest.

ACKNOWLEDGMENTS

Financial support is acknowledged from the Nelson Mandela Metropolitan University. M.R.C. thanks the University of Cape Town and the National Research Foundation (Pretoria) for financial support. P. Pohl is thanked for NMR analyses.

REFERENCES

- (1) Barton, B.; Caira, M. R.; Hosten, E. C.; McClelland, C. W. *Tetrahedron* **2013**, *69*, 8713–8723.
- (2) Seebach, D.; Beck, A. K.; Heckel, A. *Angew. Chem., Int. Ed.* **2001**, *40*, 92–138.
- (3) Barton, B.; Caira, M. R.; Hosten, E. C.; McClelland, C. W.; Weitz, S. *Chem. Commun.* **2014**, *50*, 13353–13355.
- (4) Lemière, G. L.; Dommissie, R. A.; Lepoivre, J. A.; Alderweireldt, F. C.; Hiemstra, H.; Wynberg, H.; Jones, J. B.; Toone, E. J. *J. Am. Chem. Soc.* **1987**, *109*, 1363–1370.
- (5) Tanaka, K.; Hori, K.; Tsuyuhara, S.; Motoki, S.; Shide, S.; Arakawa, R.; Caira, M. R. *Tetrahedron* **2013**, *69*, 1120–1127.
- (6) Klyne, W. *Experientia* **1956**, *15*, 119–124.
- (7) Allinger, N. L.; Freiberg, L. A. *J. Am. Chem. Soc.* **1962**, *84*, 2201–2203.
- (8) Takahashi, O.; Yamasaki, K.; Kohno, Y.; Kurihara, Y.; Ueda, K.; Umezawa, Y.; Suezawa, H.; Nishio, M. *Tetrahedron* **2008**, *64*, 2433–2440.
- (9) Hehre, W. J. *A Guide to Molecular Mechanics and Quantum Chemical Calculations*; Wavefunction, Inc.: Irvine, CA, 2003; pp 97–108.
- (10) Shan, Z.; Hu, X.; Zhou, Y.; Peng, X.; Li, Z. *Helv. Chim. Acta* **2010**, *93*, 497–503.
- (11) APEX2, SAINT, and SADABS; Bruker AXS Inc.: Madison, WI, 2010.
- (12) Sheldrick, G. M. A short history of SHELX. *Acta Crystallogr.* **2008**, *A64*, 112–122.
- (13) Hübschle, C. B.; Sheldrick, G. M.; Dittrich, B. ShelXle: a Qt graphical user interface for SHELXL. *J. Appl. Crystallogr.* **2011**, *44*, 1281–1284.
- (14) Sheldrick, G. M. *CELL_NOW*; University of Göttingen: Göttingen, Germany, 2004.